JACS
JOURNAL OF THE AMERICAN CHEMICAL SOCIETY

Communication

pubs.acs.org/JACS

Well-Defined Nanographene–Rhenium Complex as an Efficient Electrocatalyst and Photocatalyst for Selective CO_2 Reduction

Xiaoxiao Qiao,[†] Qiqi Li,[†] Richard N. Schaugaard, Benjamin W. Noffke, Yijun Liu, Dongping Li, Lu Liu, Krishnan Raghavachari, and Liang-shi Li*

Department of Chemistry, Indiana University, Bloomington, Indiana 47405, United States

Supporting Information

ABSTRACT: Improving energy efficiency of electrocatalytic and photocatalytic CO_2 conversion to useful chemicals poses a significant scientific challenge. We report on using a colloidal nanographene to form a molecular complex with a metal ion to tackle this challenge. In this work, a well-defined nanographene–Re complex was synthesized, in which electron delocalization over the nanographene and the metal ion significantly decreases the electrical potential needed to drive the chemical reduction. We show the complex can selectively electrocatalyze CO_2 reduction to CO in tetrahydrofuran at −0.48 V vs NHE, the least negative potential reported for a molecular catalyst. In addition, the complex can absorb a significant spectrum of visible light to photocatalyze the chemical transformation without the need for a photosensitizer.

Minimizing adverse environmental impacts of the increasing CO_2 in the atmosphere poses a significant scientific and societal challenge. For this purpose, electrochemical and photochemical conversions of CO_2 to fuels and other useful materials have a great potential because they can use renewable energy sources to drive the chemical transformations.[1] Despite previous efforts on various catalysts to facilitate the conversions, low energy efficiency has been a major obstacle preventing their large-scale applications.[1] To overcome this obstacle, molecular catalysts have drawn significant interest because they can direct the reactions along selected multielectron pathways[1b,e] and thus hold the promise of achieving high energy efficiency and high selectivity in the reactions. Nevertheless, strategies are still needed to decrease their catalytic overpotentials that result from the mismatch between the reduction potentials of the catalysts and those of the reactions to be catalyzed.[1b,c]

Size-dependent redox potentials and bandgaps in semiconductor nanocrystals (or "quantum dots") have been well-known[2] and have led to various optoelectronic applications.[3] In addition, semiconductor nanocrystals of various sizes have been investigated as photosensitizers for photocatalysis.[4] Upon light absorption, they supply electrons to an electrocatalyst, however do not participate in the catalyzed reactions and do not improve the energy efficiency of the electrocatalysis. Recently, we developed well-defined colloidal quantum dots of graphene,[5] a two-dimensional zero-bandgap semiconductor, and have similarly demonstrated their size-dependent optical and redox properties.[6] Herein we report on the use of colloidal graphene quantum dots, or nanographenes, as a ligand for metal ions for electrocatalytic and photocatalytic CO_2 reduction. The tightly controlled nanographene structures enable us to make a well-defined molecular nanographene–rhenium complex with the nanographene as an integral part of the catalyst. We show electron delocalization over the ligand and the metal ion significantly decrease the electrical potential needed for the CO_2 reduction. As a result, the complex electrocatalytically reduces CO_2 selectively to CO in tetrahydrofuran (THF) at −0.48 V vs NHE, the least negative potential reported so far for a molecular catalyst. In addition, incorporation of the nanographene enables the complex to absorb a significant spectrum of visible light to drive photocatalytic CO_2 reduction.

$Re^I(\alpha\text{-diimine})(CO)_3X$ complexes (where X = Cl^- or Br^-) are among the best studied electrocatalysts for CO_2 reduction and the mechanisms have been extensively studied.[7] As shown with *fac*-Re^I(bipyridine)$(CO)_3Cl$ (shortened as [Rebpy] herein), to reduce CO_2 the complexes first undergo a one-electron reduction at the bpy ligand ("ligand-centered", −1.11 V vs NHE in acetonitrile), followed by another one-electron reduction primarily at the metal center ("metal-centered", at −1.48 V). The latter results in rapid loss of Cl^- and produces the active form of catalyst $[Re(bpy)(CO)_3]^-$ that binds to CO_2 and converts it to CO with protons present. Alternatively, the loss of Cl^- may occur after the first reduction, leading to a much slower reduction pathway.[7b] In dimethylformamide/water mixture (vol./vol. 9/1), the [Rebpy] upon the second reduction can electrocatalytically convert CO_2 exclusively to CO, with faradaic efficiency of 98%.[7a] However, because of the required metal-centered reduction, previous studies have shown no correlation between the ligand properties and the catalytic properties of the complexes.[8] As a result, there has not yet been a general strategy for improvement of the energy efficiency of the electrocatalyzed reaction.

We synthesized nanographenes as the diimine ligand (e.g., **1** in Scheme 1) to tune the reduction potentials of the $Re^I(\alpha$-

Scheme 1. Structures of Nanographenes 1, 2, and Complex 3

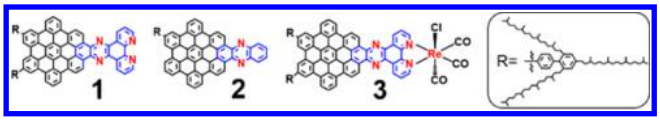

Received: December 5, 2016

DOI: 10.1021/jacs.6b12530
J. Am. Chem. Soc. XXXX, XXX, XXX−XXX

diimine) $(CO)_3X$ complexes for improved energy efficiency in CO_2 reduction. Our previous studies have shown, as a result of quantum confinement in the two-dimensional semiconductor, nanographenes have size-dependent optical and redox properties.[6] In particular, nanographene **2** containing a pyrazinyl moiety can undergo a proton-coupled two-electron reduction in alkaline aqueous electrolytes to electrocatalyze the oxygen reduction reaction, another kinetically sluggish multielectron reaction.[9] We anticipate such a structure may serve as electron storage for multielectron CO_2 reductions as well, and thus we synthesized nanographene **1** similar in structure with a phenanthroline moiety to form complex **3**. Crucial for our studies are the peripheral trialkylphenyl groups (R-group in Scheme 1) that make **1**–**3** soluble in organic solvents such as toluene and THF. Because of their 3-dimensional arrangement, the alkyl chains form a cage around the conjugated core of the nanographene to effectively prevent aggregation due to $\pi-\pi$ stacking.[5a,10]

Synthesis of **1** is outlined in Scheme 2, following a method we previously developed for **2** with some modifications.[6a]

Scheme 2. Synthesis of 1[a]

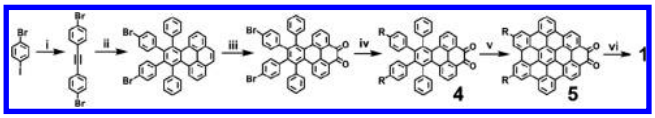

[a]Reaction conditions: (i) CaC_2, $Pd(OAc)_2$, PPh_3, TEA, CH_3CN, 20 °C; (ii) 9,11-diphenyl-10*H*-cyclopenta[e]pyren-10-one, diphenyl ether, 240 °C; (iii) $NaIO_4$, $RuCl_3$, dichloromethane, CH_3CN, H_2O, 40 °C; (iv) 4-(2′,4′,6′-trialkylphenyl)phenylborate, $Pd(PPh_3)_4$, K_2CO_3, toluene, ethanol, H_2O, 80 °C; (v) $FeCl_3$, dichloromethane, CH_3NO_2, 20 °C; (vi) 1,10-phenanthroline-5,6-diamine, pyridine, reflux.

Briefly, we start with 1-bromo-4-iodobenzene to produce an α-diketone-functionalized polyphenylene derivative (**4**). **4** and its precursors are purified with silica gel chromatography and characterized with standard organic characterization techniques (see SI). Treatment of **4** with an excess of iron(III) chloride in a dichloromethane/nitromethane mixture leads to **5**. It was then purified with repetitive dissolution in toluene and precipitation with methanol to remove all iron species, confirmed with bipyridine added to the supernatants as a colorimetric indicator. The structure of **5** is confirmed with isotope-resolved MALDI-mass spectroscopy (MS), consistent with the simulated spectrum for the molecular formula $C_{188}H_{272}O_2$ and showing excellent size uniformity (Figure 1a). Subsequently, **5** undergoes two quantitative reactions, first with 1,10-phenanthroline-5,6-diamine to yield **1**, and then with excess of $Re(CO)_5Cl$ in hot toluene to yield **3**. The reactions were monitored with infrared (IR) spectroscopy (Figure 1b), in which complete conversion of **5** to **1** is accompanied by disappearance of the carbonyl stretching (1663 cm^{-1}) and conversion of **1** to **3** by three CO peaks showing the *fac*-geometry (2024, 1921, and 1885 cm^{-1}, respectively). Again, **1** and **3** were purified with repetitive dissolution in toluene and precipitation with methanol to remove small molecule species. NMR spectroscopy was not able to resolve the aromatic protons in **5**, **1**, or **3** even at elevated temperature, because of their large size and slow tumbling dynamics.[5b,6b,10b]

Electrochemical studies of **3** were carried out in dry THF, Bu_4NPF_6 (0.1 M) as electrolyte, glassy carbon as working electrode, and $Ag/AgNO_3$ (0.01 M in acetonitrile) as reference

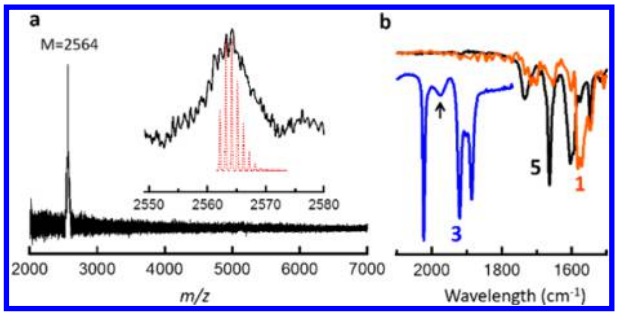

Figure 1. (a) MALDI-MS spectrum of **5**. (Inset) Isotope resolved spectrum (black solid curve) consistent with simulated spectrum (red dotted curve) with anticipated molecular formula $C_{188}H_{272}O_2$. (b) IR spectroscopy monitoring conversion of **5** (black) to **1** (orange) and then to **3** (blue). The spectra were obtained with solid films of **5** and **1**, and a solution of **3** in THF. The sharp peak for **5** at 1663 cm^{-1} is due to the diketone moiety. In the spectrum of **3**, the three sharp peaks (2024, 1921, and 1885 cm^{-1}, respectively) are due to the three CO ligands in *fac*-geometry. The peak marked with an arrow (1973 cm^{-1}) is residual absorption of THF.

electrode. The black solid curve in Figure 2 shows the cyclic voltammetry (CV) curve obtained for **3** in dry THF (0.1 mM)

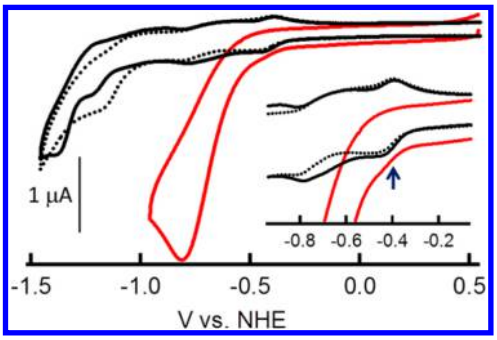

Figure 2. CV measurements of 0.1 mM solution of **3** in dry THF (50 mV/s). (Inset) Zoom-in of the current rising edge, with the arrow marking the equilibrium potential of the first reduction (−0.40 V). Black solid curve: in dry THF saturated with argon (1 atm, same below). Black dotted curve: in dry THF saturated with CO_2. Red solid curve: in dry THF/methanol mixture (vol./vol. 95/5) saturated with CO_2. The electrochemical potentials were measured with $Ag/AgNO_3$ (0.01 M in acetonitrile) as reference electrode and converted to values vs NHE.

saturated with argon (1 atm, 50 mV/s), with the potentials converted to values vs NHE for comparison with previous studies. The cathodic scan reveals a series of reduction peaks, at −0.43, −0.78, −1.19, and −1.31 V, respectively. Measurements at various scan rates show the first reduction (−0.43 V) as a reversible one-electron reduction in the time scale of the CV measurements, for which the positions of the reduction and the oxidation peaks remain invariant and 60 mV apart (Figure S1). The reduction at −0.78 V is an irreversible one-electron process, indicating electrochemically triggered reactions. Nevertheless, the two reductions occur at potentials considerably less negative than those of [Rebpy] (ca. −1.11 and −1.48 V in acetonitrile, respectively[8b]), suggesting, because of their dependence on size of the diimine ligands, significant delocalization of the added electrons in the ligand. This is supported by our DFT calculations (Figure 3). Upon the first reduction of **3**, electron density increment occurs predominantly in the nanographene ligand (Figure 3a), and upon the

DOI: 10.1021/jacs.6b12530
J. Am. Chem. Soc. XXXX, XXX, XXX−XXX

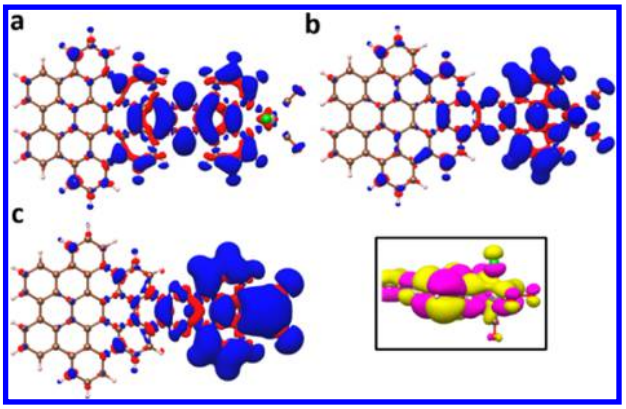

Figure 3. Calculated electron density difference plots upon the first (a), second (b) reduction of **3**, and subsequent dechlorination (c). The blue color represents electron density increment and red the decrement. Inset: side view of the highest (singly) occupied molecular orbital of 3^{2-} around the metal center, highlighting the Cl−Re σ^* component. Dechlorination of 3^{2-} according to our calculations is thermodynamically favored, leading to significant shift of electron density from the ligand to the metal center (c). Here the Cl atom is marked green, and Re marked gray. The isovalue for all the electron density difference is 0.005 au, and for the orbital plot 0.01 au.

second reduction in the ligand as well as the metal center (Figure 3b). The reductions of **3** at more negative potentials appear to be irreversible and have not been investigated.

Complex **3** can electrocatalyze CO_2 reduction with a Brønsted acid present at a potential significantly more positive than [Rebpy]. In Figure 2, the black dotted curve is the CV curve for **3** in dry THF (0.1 mM) saturated with CO_2 (1 atm, 50 mV/s), showing little difference from the black solid curve. When a Brønsted acid such as methanol is added, a substantially enhanced current is observed upon the second reduction of **3**, indicating catalytic reduction of CO_2. This is demonstrated by the red solid curve in Figure 2, the CV curve for **3** in a THF/methanol mixture (vol./vol. 95/5) saturated with CO_2 (1 atm), which shows the onset of the catalytic current at ca. −0.48 V. Bulk electrolysis on such a solution with potential held at −0.86 V and subsequent GC analysis show CO as the only product with no H_2 detected (see SI). Turnover number was found to be 270 within a 2-h duration, with a faradaic efficiency of 96%.

The onset potential of the CO_2 to CO conversion catalyzed by **3**, i.e., −0.48 V vs NHE, is nearly 0.8 V more positive than that for [Rebpy] and is the least negative reported among molecular catalysts (see Table S1 for comparisons).[11] This is possible because delocalization of the second electron added over both the ligand and the metal center (Figure 3b) makes 3^{2-} more readily generated, in sharp contrast with [Rebpy] in which the second reduction is metal-centered. The onset potential is even less negative than the equilibrium potential for the reaction in neutral aqueous solution (−0.53 V vs NHE). However, this does not contradict thermodynamics. In organic solvents the equilibrium potential is significantly more positive (e.g., by +0.72 V in acetonitrile).[12] In addition, concentrations of the solutes in our experiments deviate considerably from the standard states.

To understand the activation of the catalyst, we conducted DFT calculations on the reactions of the two-electron reduction intermediate 3^{2-}. In particular we investigated its propensity to lose Cl^-, a key step in CO_2 reduction at the metal center. Because the highest (singly) occupied molecular orbital of 3^{2-} contains significant component of the Cl−Re σ^* orbital (Figure 3, inset, details in SI),[13] loss of Cl^- from 3^{2-} is slightly endothermic and thermodynamically spontaneous (ΔH^0 = +10.3 kcal/mol and ΔG^0 = −0.6 kcal/mol, with 1 M as the standard states of the solutes). With $[Cl^-]$ in our experiments less than 0.1 mM, the loss of Cl^- is highly favored (ΔG < −6.1 kcal/mol). The dechlorination product, now with a five-coordinate Re, has electron density significantly shifted toward the metal center (Figure 3c). The resultant electron distribution highly resembles the active form $[Re(bpy)(CO)_3]^-$ identified for the [Rebpy] catalyst,[7e] and presumably is the active form of catalyst for **3** that subsequently forms adducts with CO_2 and enables its selective reduction.[7d] Similarly, protons will be needed in protonation of the CO_2-adducts and subsequent reactions, which will be further investigated. Our calculations also show loss of Cl^- from 3^- is unfavored (ΔG^0 = +20.6 kcal/mol, SI), explaining the reversible first reduction of **3**. Our calculations are performed based on unrestricted Kohn−Sham density functional theory with the quantum chemical package ORCA 3.0.3[14] using the hybrid exchange-correlation functional B3LYP (see SI). A conductor-like continuum solvation model COSMO[15] is used to estimate free energy of solvation in THF (ε = 7.25).

The ability of **3**, because of ligand **1**, to absorb visible light makes it very attractive for potential photocatalytic activity. The absorption spectra of **1**−**3** are shown in Figure 4, extending up

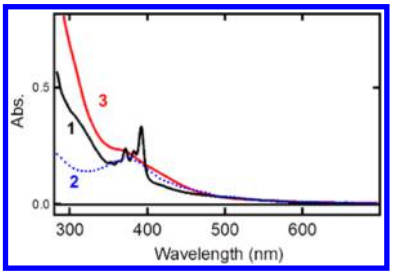

Figure 4. Absorption spectra of **1**−**3** in THF.

to 600 nm. The most notable features in the spectrum of **1** are a series of well-resolved vibronic structures between 350 and 400 nm and a long tail from 400 to 600 nm, the former resembling the spectrum of dipyridophenazine (marked blue in **1**, Scheme 1)[16] and the latter that of **2**. Chelation in **3** significantly broadens the vibronic structures, yet no distinct metal-to-ligand-charge-transfer transition band is observed. Indeed, our subsequent photochemical studies show that **3** can photocatalyze the CO_2 reduction with visible light. The photochemical studies were conducted by illuminating a CO_2-saturated solution of **3** and an excess of triethanolamine (TEOA) in dry THF. The light source is a 100 W tungsten lamp with a long-pass filter at 490 nm cutoff. GC analysis shows CO as the only product, with a turnover number of 48, comparable with reported values for [Rebpy].[8a] Nevertheless, the extended absorption spectrum of **3** eliminates the need for photosensitizers in the cases of [Rebpy] and derivatives[17] for visible-light-driven photocatalysis. The origin of the second electron to reduce each CO_2 molecule[17a] is not yet clear and will be investigated in the future.

In summary, by using the nanographene as a ligand to form a complex with rhenium ion, we show significantly less negative potential for electrocatalytic CO_2 reduction as well as visible-light-driven photocatalytic CO_2 reduction without the need for

DOI: 10.1021/jacs.6b12530
J. Am. Chem. Soc. XXXX, XXX, XXX−XXX

a photosensitizer. Because of the size-dependent electrochemical and optical properties of nanographenes,[6] we anticipate employing larger nanographene ligands will further decrease the reduction overpotential. Nevertheless, the labilization of the axial ligand Cl^- determines whether the ligand-centered reductions can lead to fast CO_2 reduction; how it depends on the size of the ligands remains to be investigated.[13a] In particular, in a recent work the same Re-containing moiety was covalently linked to a glassy carbon electrode yet did not result in improvement in the CO_2 reduction potential.[18] Work to replace Re with Mn,[19] a far more earth-abundant metal, is in progress.

■ ASSOCIATED CONTENT

Supporting Information

The Supporting Information is available free of charge on the ACS Publications website at DOI: 10.1021/jacs.6b12530.

Synthesis and characterization of compounds, electrochemical and photochemical measurements, details of theoretical calculations (PDF)

■ AUTHOR INFORMATION

Corresponding Author

*li23@indiana.edu

ORCID

Xiaoxiao Qiao: 0000-0001-7053-8162

Yijun Liu: 0000-0001-9227-6781

Krishnan Raghavachari: 0000-0003-3275-1426

Liang-shi Li: 0000-0001-7566-8492

Author Contributions

†These authors contributed equally to this work.

Notes

The authors declare no competing financial interest.

■ ACKNOWLEDGMENTS

This work was supported by a seed grant from the Indiana University. We also acknowledge the financial support of the National Science Foundation (grants CHE-1266154 and CBET-1610712). We thank Erin Martin for assistance with the bulk electrolysis measurements.

■ REFERENCES

(1) (a) Whipple, D. T.; Kenis, P. J. A. *J. Phys. Chem. Lett.* **2010**, *1*, 3451. (b) Morris, A. J.; Meyer, G. J.; Fujita, E. *Acc. Chem. Res.* **2009**, *42*, 1983. (c) Benson, E. E.; Kubiak, C. P.; Sathrum, A. J.; Smieja, J. M. *Chem. Soc. Rev.* **2009**, *38*, 89. (d) Kumar, B.; Llorente, M.; Froehlich, J.; Dang, T.; Sathrum, A.; Kubiak, C. P. *Annu. Rev. Phys. Chem.* **2012**, *63*, 541. (e) Jones, J.-P.; Surya Prakash, G. K.; Olah, G. A. *Isr. J. Chem.* **2014**, *54*, 1451. (f) White, J. L.; et al. *Chem. Rev.* **2015**, *115*, 12888. (g) Appel, A. M.; et al. *Chem. Rev.* **2013**, *113*, 6621.

(2) (a) Efros, A. L.; Rosen, M. *Annu. Rev. Mater. Sci.* **2000**, *30*, 475. (b) Brus, L. E. *Appl. Phys. A: Solids Surf.* **1991**, *53*, 465.

(3) (a) Talapin, D. V.; Lee, J.-S.; Kovalenko, M. V.; Shevchenko, E. V. *Chem. Rev.* **2010**, *110*, 389. (b) Kovalenko, M. V.; et al. *ACS Nano* **2015**, *9*, 1012.

(4) (a) Han, Z.; Qiu, F.; Eisenberg, R.; Holland, P. L.; Krauss, T. D. *Science* **2012**, *338*, 1321. (b) Wu, K.; Lian, T. *Chem. Soc. Rev.* **2016**, *45*, 3781.

(5) (a) Li, L.-S.; Yan, X. *J. Phys. Chem. Lett.* **2010**, *1*, 2572. (b) Yan, X.; Li, B.; Li, L.-S. *Acc. Chem. Res.* **2013**, *46*, 2254.

(6) (a) Li, Q.; Zhang, S.; Dai, L.; Li, L.-S. *J. Am. Chem. Soc.* **2012**, *134*, 18932. (b) Yan, X.; Cui, X.; Li, L.-S. *J. Am. Chem. Soc.* **2010**, *132*, 5944. (c) Yan, X.; Li, B.; Cui, X.; Wei, Q.; Tajima, K.; Li, L.-S. *J. Phys. Chem. Lett.* **2011**, *2*, 1119.

(7) (a) Hawecker, J.; Lehn, J.-M.; Ziessel, R. *J. Chem. Soc., Chem. Commun.* **1984**, 328. (b) Sullivan, B. P.; Bolinger, M.; Conrad, D.; Vining, W. J.; Meyer, T. J. *J. Chem. Soc., Chem. Commun.* **1985**, 1414. (c) Hawecker, J.; Lehn, J.-M.; Ziessel, R. *Helv. Chim. Acta* **1986**, *69*, 1990. (d) Riplinger, C.; Sampson, M. D.; Ritzmann, A. M.; Kubiak, C. P.; Carter, E. A. *J. Am. Chem. Soc.* **2014**, *136*, 16285. (e) Grice, K. A.; Kubiak, C. P. *Adv. Inorg. Chem.* **2014**, *66*, 163.

(8) (a) Kurz, P.; Probst, B.; Spingler, B.; Alberto, R. *Eur. J. Inorg. Chem.* **2006**, *2006*, 2966. (b) Smieja, J. M.; Kubiak, C. P. *Inorg. Chem.* **2010**, *49*, 9283.

(9) (a) Li, Q.; Noffke, B.; Wang, Y.; Menezes, B.; Peters, D. G.; Raghavachari, K.; Li, L.-S. *J. Am. Chem. Soc.* **2014**, *136*, 3358. (b) Li, Q.; Noffke, B. W.; Liu, Y.; Li, L.-S. *Curr. Opin. Colloid Interface Sci.* **2015**, *20*, 346.

(10) (a) Yan, X.; Li, L.-S. *J. Mater. Chem.* **2011**, *21*, 3295. (b) Yan, X.; Cui, X.; Li, B.; Li, L.-S. *Nano Lett.* **2010**, *10*, 1869.

(11) (a) Sampson, M. D.; Kubiak, C. P. *J. Am. Chem. Soc.* **2016**, *138*, 1386. (b) Azcarate, I.; Costentin, C.; Robert, M.; Savéant, J.-M. *J. Am. Chem. Soc.* **2016**, *138*, 16639.

(12) Pegis, M. L.; Roberts, J. A. S.; Wasylenko, D. J.; Mader, E. A.; Appel, A. M.; Mayer, J. M. *Inorg. Chem.* **2015**, *54*, 11883.

(13) (a) Klein, A.; Vogler, C.; Kaim, W. *Organometallics* **1996**, *15*, 236. (b) Vlcek, J. A. In *Electron Transfer in Chemistry*; Balzani, V., Ed.; Wiley: Weinheim, 2001.

(14) Neese, F. *WIRES Comput. Mol. Sci.* **2012**, *2*, 73.

(15) Klamt, K.; Schüürman, G. *J. Chem. Soc., Perkin Trans. 2* **1993**, 799.

(16) Dyer, J.; et al. *Photochem. Photobiol. Sci.* **2003**, *2*, 542.

(17) (a) Takeda, H.; Ishitani, O. *Coord. Chem. Rev.* **2010**, *254*, 346. (b) Sahara, G.; Ishitani, O. *Inorg. Chem.* **2015**, *54*, 5096.

(18) Oh, S.; Gallagher, J. R.; Miller, J. T.; Surendranath, Y. *J. Am. Chem. Soc.* **2016**, *138*, 1820.

(19) Bourrez, M.; Molton, F.; Chardon-Noblat, S.; Deronzier, A. *Angew. Chem., Int. Ed.* **2011**, *50*, 9903.

DOI: 10.1021/jacs.6b12530
J. Am. Chem. Soc. XXXX, XXX, XXX−XXX